Itemized List of Supplemental Material

Supplemental Figure 1: Relates to Figure 2. Provides additional validation of the ChIP-seq results shown in Fig. 2.

Supplemental Figure 2: Relates to Figure 3. Provides further characterization of the phenotypic consequences of UTX knockdown in T-ALL presented in Fig. 3.

Supplemental Figure 3: Relates to Figure 3. Provides further characterization of the phenotypic consequences of UTX knockdown in T-ALL presented in Fig. 3. Specifically, it provides visualization of the genes GO terms enriched upon UTX knockdown as analyzed by RNA-seq.

Supplemental Figure 4: Relates to Figure 4. Provides further characterization of the effect of GSK-J4 in TAL1-positive and TAL1-negative T-ALL.

Supplemental Figure 5: Relates to Figure 5. Provides further assessment of the effect of GSK-J4 administration in mice.

Supplemental Figure 6: Relates to Figure 2. Provides further characterization of the role of UTX in the PF382 T-ALL cell line that expresses UTX from one allele only.

Supplemental Table 1: Relates to Figure 1. Provides the full list of TAL1-interacting proteins identified by mass spectrometry.

Supplemental Table 2: Relates to Figures 2 and 3. Provides the full list of TAL1/UTX co-bound genes identified by ChIP-seq, and the full list of GO terms enriched upon UTX knockdown.

Supplemental Material and Methods

Supplemental References

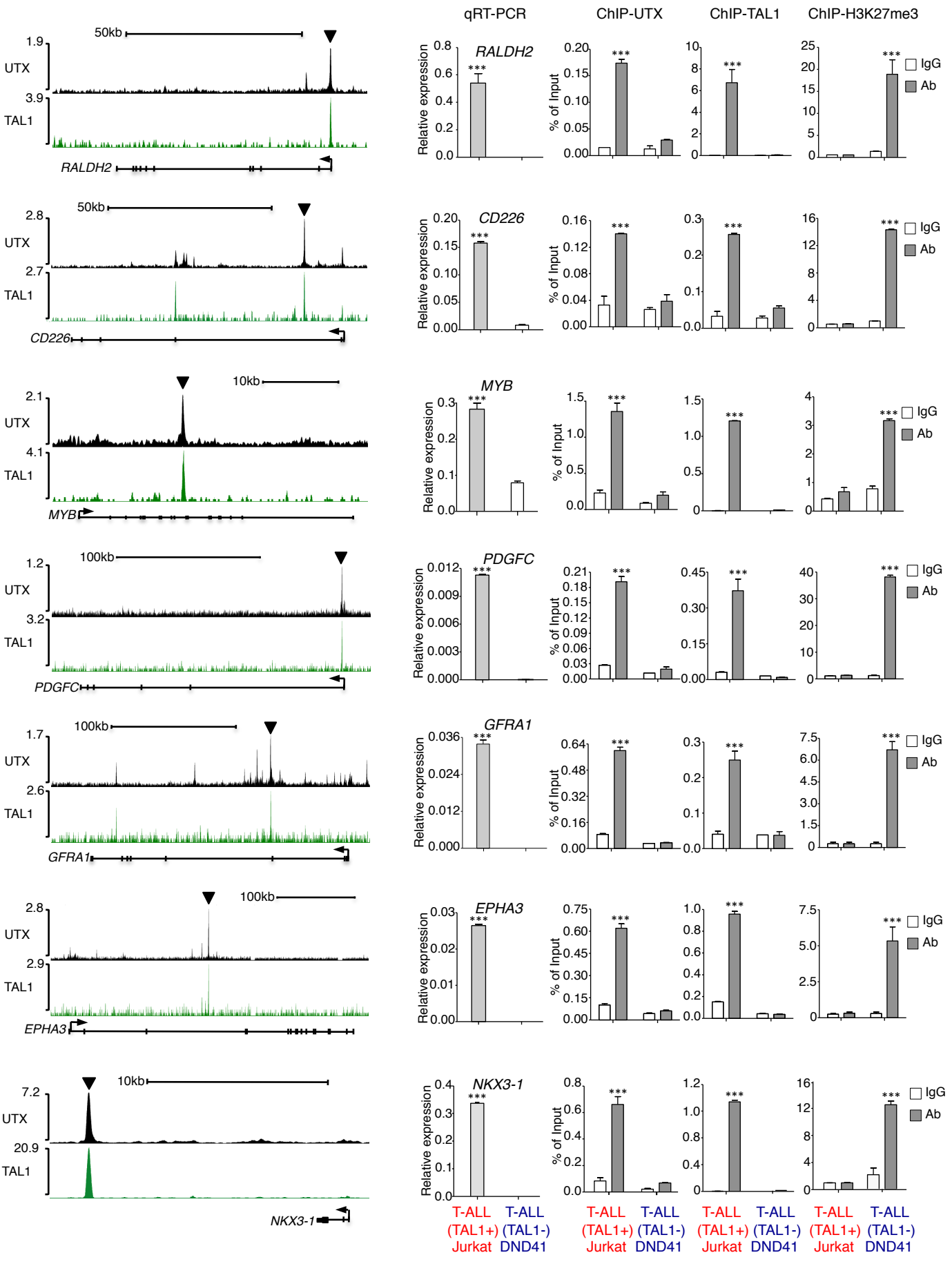
qRT-PCR
ChIP-UTX
ChIP-TAL1
ChIP-H3K27me3
50kb
1.9
UTX
3.9
TAL1
RALDH2
Relative expression
% of Input
***
IgG
Ab
50kb
2.8
UTX
2.7
TAL1
CD226
10kb
2.1
UTX
4.1
TAL1
MYB
100kb
1.2
UTX
3.2
TAL1
PDGFC
100kb
1.7
UTX
2.6
TAL1
GFRA1
100kb
2.8
UTX
2.9
TAL1
EPHA3
10kb
7.2
UTX
20.9
TAL1
NKX3-1
T-ALL (TAL1+) Jurkat
T-ALL (TAL1-) DND41

Supplemental Figure 1. UTX-mediated activation of TAL1 target genes in T-ALL

Left panels: ChIP-seq density plots (normalized by reads per million mapped reads) for UTX and TAL1 at the indicated gene loci in TAL1-positive Jurkat T-ALL cells. Right panels: Validation of differential expression, UTX and TAL1 binding as well as H3K27me3 enrichment at the indicated gene loci in TAL1-positive Jurkat vs. TAL1-negative DND41 T-ALL cells.

qRT-PCR values are expressed relative to the internal control *ß2M* +/- s.d. (n=3).

ChIP-qPCR values are expressed as a fraction of input +/- s.d. (n=3).

***$p < 0.001$.

A

Cell line ID	Age / Sex	Origin	TAL 1 expression *
CEM / C1	4 / F	ATCC	Positive
PF-382	6 / F	DSMZ	Positive
Jurkat	14 / M	Invitrogen	Positive
DND-41	13 / M	DSMZ	Negative
SUP-T1	8 / M	ATCC	Negative

B

Patient ID	Age / Sex	Stage of T-ALL	Reference	TAL 1 expression *
M18	6 / M	Medullary T	Armstrong et al. 2009	Positive
M69	12 / F	Medullary T	Gerby et al. 2011	Positive
08h125	24 / F	Pre-T	Simon et al. 2012	Positive
03h005	18 / M	Medullary T	Simon et al. 2012	Positive
08h028	52 / F	Pro-T	Simon et al. 2012	Negative
05h129	18 / M	Cortical T	Simon et al. 2012	Negative

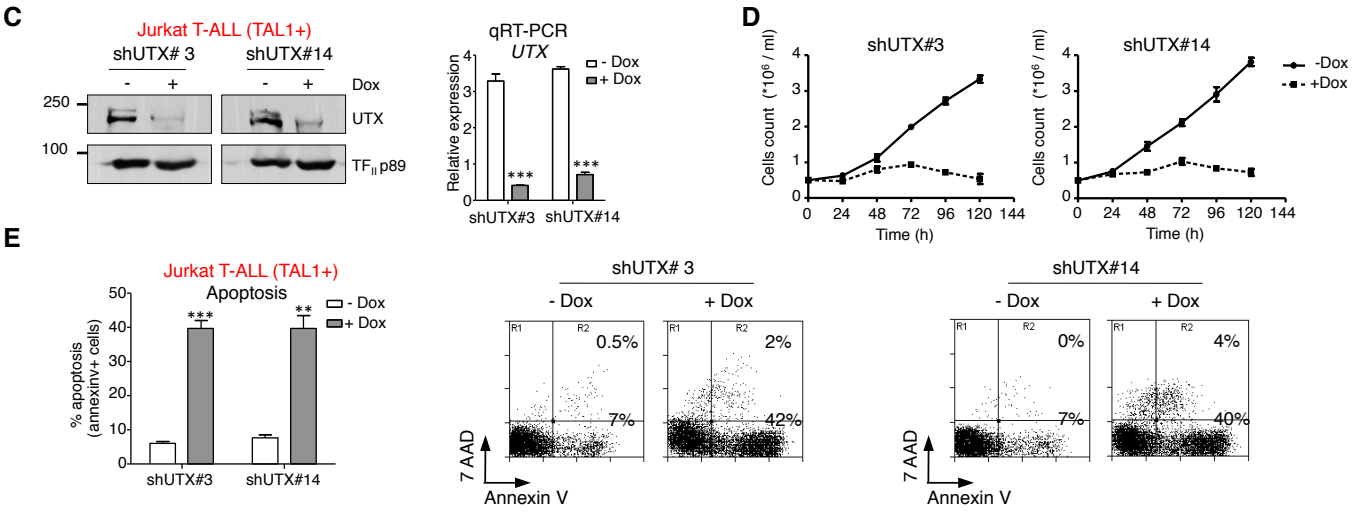

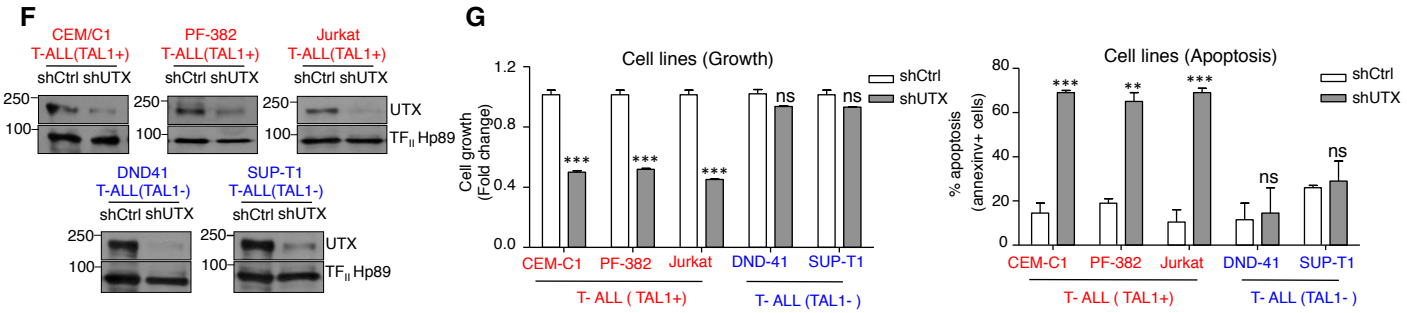

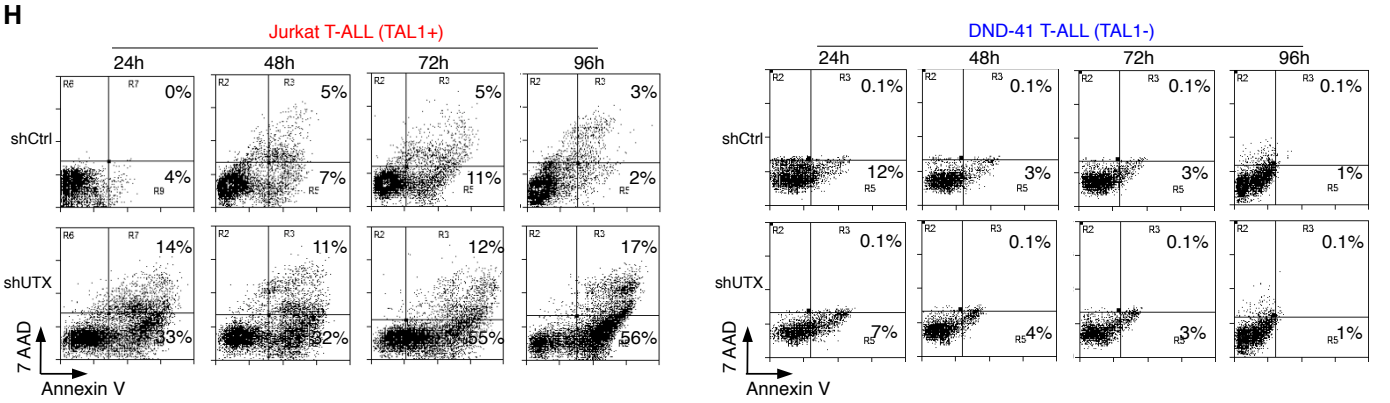

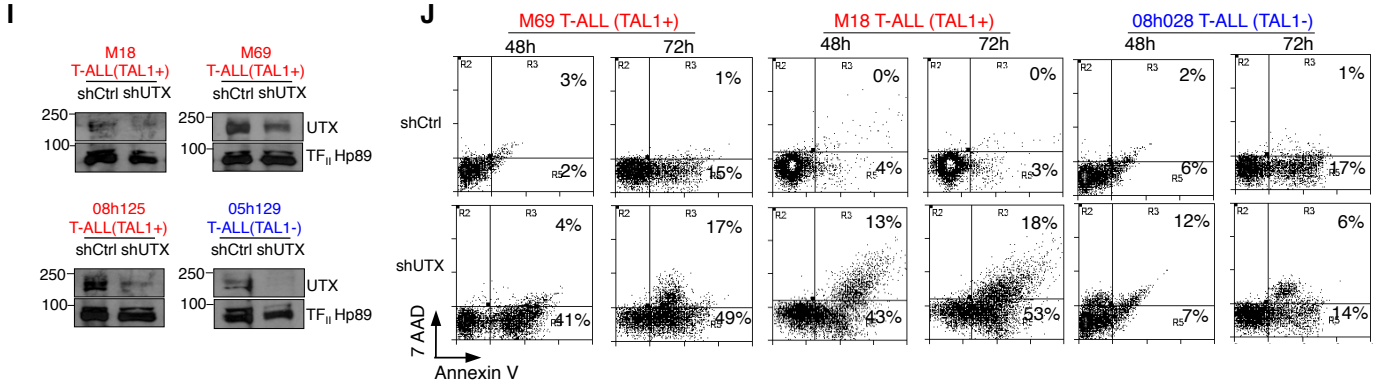

Supplemental Figure 2. UTX is involved in leukemia maintenance of TAL1-positive but not TAL1-negative T-ALL

A, Characteristics of T-ALL cell lines

B, Characteristics of T-ALL patients

A, **B**, * TAL1 expression analyzed by Western blot (Fig. 3A)

C, Dox-mediated expression of anti-UTX shRNAs (shUTX#3 and shUTX#14) in Jurkat cells induces UTX knockdown as seen by Western blot (left) and qRT-PCR (right). Left: Western blots shown as a representative examples of three biological replicates. Molecular masses (in kDa) are indicated. Right: qRT-PCR results are presented as mean values relative to the internal control *ß2M* +/- s.d (n=3). ***p < 0.001.

D, UTX knockdown by Dox induction leads to a profound defect in the growth of Jurkat cells. Viable cells were counted and the data are presented as mean +/- s.e.m. (n=3).

E, UTX knockdown by Dox induction induces apoptosis of Jurkat cells. Apoptosis is reported as the percentage of Annexin V positive cells. Data are shown as mean +/- s.e.m. (n=3). **p < 0.01; ***p < 0.001. Representative FACS plots are shown on the right.

F, Knockdown of UTX by lentiviral delivery of anti-UTX shRNA in T-ALL cell lines. Western blots shown as representative examples of three biological replicates. Molecular masses (in kDa) are indicated.

G, Left panel: UTX knockdown decreases the growth of TAL1-positive but not TAL1-negative T-ALL cell lines. The fold-change of viable cells with UTX knockdown (shUTX) relative to viable cells without knockdown (shCtrl) is reported as mean +/- s.e.m. (n=3). Right panel: UTX knockdown triggers apoptosis in TAL1-positive but not

TAL1-negative T-ALL cell lines. Apoptosis is reported as the percentage of Annexin V positive cells. Data are shown as mean +/- s.e.m. (n=3). **p < 0.01; ***p < 0.001; ns, not significant.

H, FACS plots measuring Annexin V staining are shown at different time-points after UTX knockdown in Jurkat and DND41 T-ALL cell lines. Representative examples of three biological replicates are shown. Mean data for these cell lines and other cell lines are presented in panel G.

I, Knockdown of UTX by lentiviral delivery of anti-UTX shRNA in primary blasts from T-ALL patients. Western blots shown as representative examples of three biological replicates. Molecular masses (in kDa) are indicated.

J, FACS plots measuring Annexin V staining after UTX knockdown in primary blasts from the indicated T-ALL patients. Representative examples of three biological replicates are shown. Mean data for these patients and additional patients are presented in Fig. 3D.

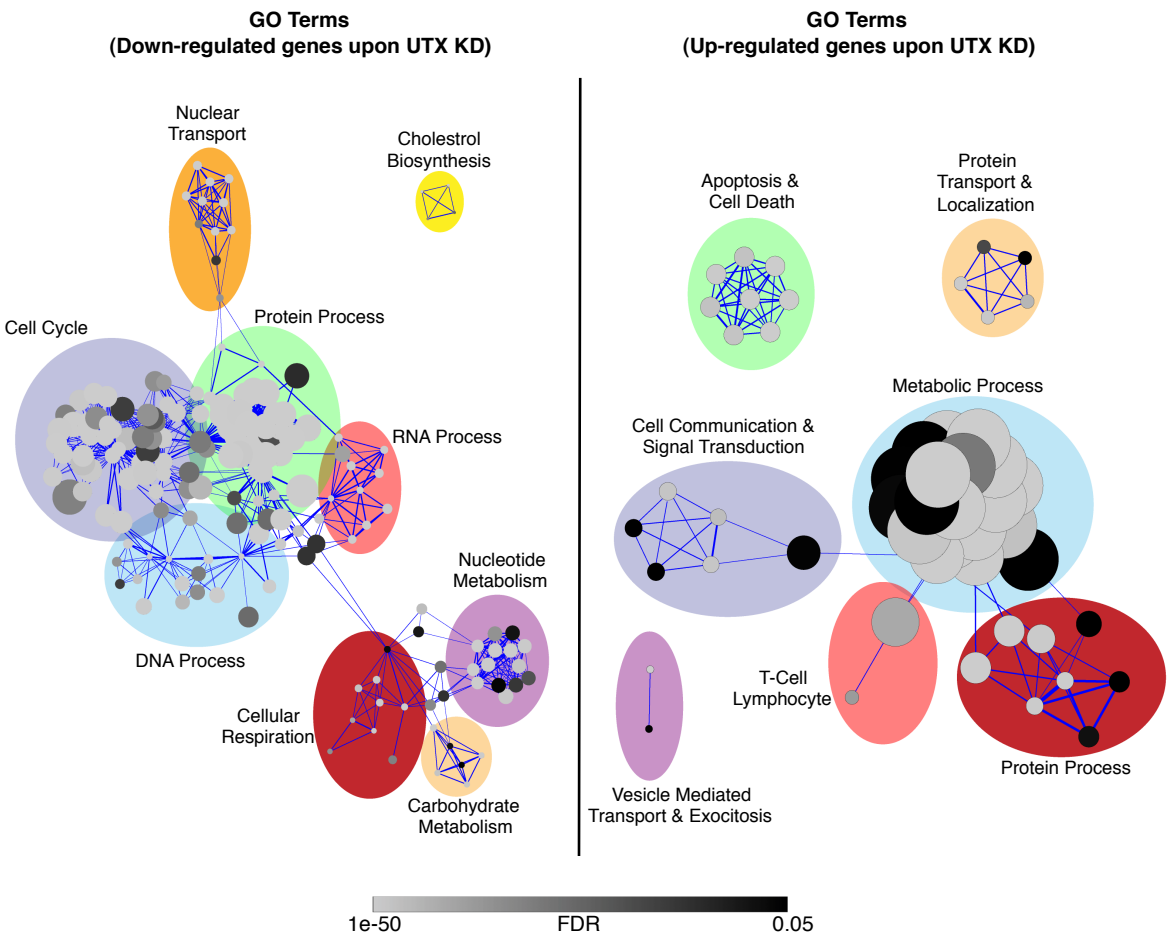
GO Terms
(Down-regulated genes upon UTX KD)
Nuclear Transport
Cholestrol Biosynthesis
Cell Cycle
Protein Process
RNA Process
Nucleotide Metabolism
DNA Process
Cellular Respiration
Carbohydrate Metabolism
GO Terms
(Up-regulated genes upon UTX KD)
Apoptosis & Cell Death
Protein Transport & Localization
Metabolic Process
Cell Communication & Signal Transduction
T-Cell Lymphocyte
Protein Process
Vesicle Mediated Transport & Exocitosis
1e-50
FDR
0.05

Supplemental Figure 3. Changes in gene expression upon UTX knockdown in TAL1-positive T-ALL

Enrichment map of biological processes that are up- or down- regulated upon UTX knockdown in TAL1+ Jurkat T-ALL cells. Genes that are significantly up- or down-regulated (adjusted p-value ≤ 0.05) were identified by RNA-seq, analyzed by Gene Ontology (GO), and visualized using the EnrichmentMap plugin in Cytoscape. Nodes represent enriched biological processes (BP) terms with node-size being proportional to gene set size and node color variations (from grey to black) being proportional to the false discovery rate (FDR) of each node, as indicated. Edges represent associations between enriched processes. Clusters of functionally related gene-sets were circled and manually labeled.

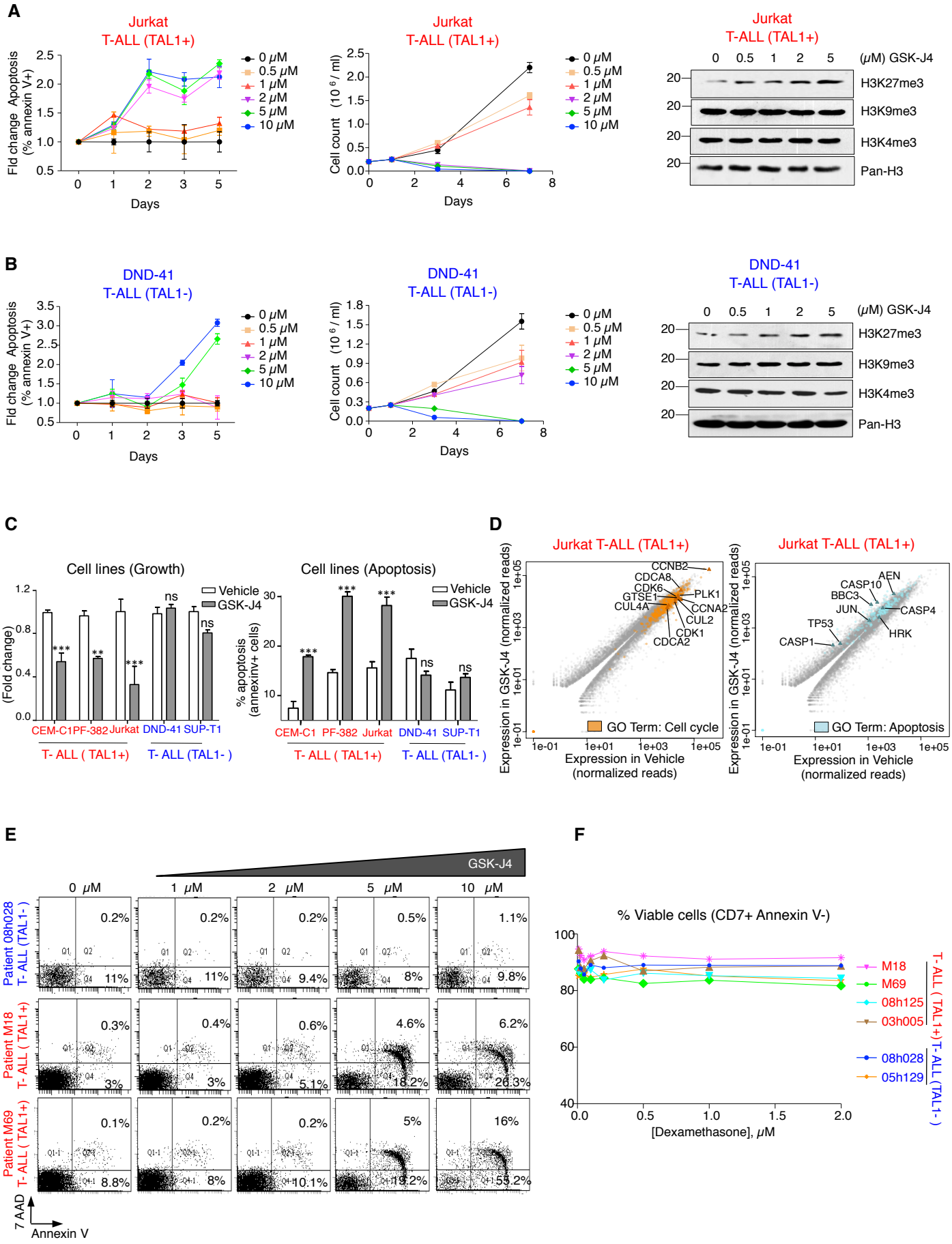
A
Jurkat
T-ALL (TAL1+)
Fld change Apoptosis (% annexin V+)
Days
0 μM
0.5 μM
1 μM
2 μM
5 μM
10 μM
Cell count (10 6 / ml)
(μM) GSK-J4
H3K27me3
H3K9me3
H3K4me3
Pan-H3
B
DND-41
T-ALL (TAL1-)
C
Cell lines (Growth)
Cell growth (Fold change)
Vehicle
GSK-J4
CEM-C1 PF-382 Jurkat DND-41 SUP-T1
T- ALL (TAL1+)
T- ALL (TAL1-)
Cell lines (Apoptosis)
% apoptosis (annexinv+ cells)
D
Jurkat T-ALL (TAL1+)
Expression in GSK-J4 (normalized reads)
Expression in Vehicle (normalized reads)
CCNB2
CDCA8
CDK6
GTSE1
CUL4A
PLK1
CCNA2
CUL2
CDK1
CDCA2
GO Term: Cell cycle
AEN
CASP10
BBC3
JUN
CASP4
TP53
HRK
CASP1
GO Term: Apoptosis
E
GSK-J4
0 μM
1 μM
2 μM
5 μM
10 μM
Patient 08h028 T- ALL (TAL1-)
Patient M18 T- ALL (TAL1+)
Patient M69 T- ALL (TAL1+)
7 AAD
Annexin V
F
% Viable cells (CD7+ Annexin V-)
[Dexamethasone], μM
M18
M69
08h125
03h005
08h028
05h129
T- ALL (TAL1+)
T- ALL (TAL1-)

Supplemental Figure 4. Dose-dependent killing of TAL1-positive T-ALL by GSK-J4

A, **B**, The TAL1-positive T-ALL cell line Jurkat (**A**) is more sensitive to GSK-J4 treatment than the TAL1-negative cell line DND41 (**B**). Left panels: Dose-dependent effect of GSK-J4 on the induction of apoptosis. Data are presented as mean values of the percentage of Annexin V-positive cells +/- s.e.m. (n=3). Middle panels: Dose-dependent effect of GSK-J4 on cell growth. Data are presented as mean values of viable cells concentration +/- s.e.m. (n=3). Right panels: Dose-dependent increase in global levels of H3K27me3 upon GSK-J4 treatment. Western blots are representative of three biological replicates. Molecular masses (in kDa) are indicated. 2 μM was determined to be the optimal concentration of GSK-J4 for discriminating between TAL1-positive and TAL1-negative T-ALL cell lines.

C, GSK-J4 (2μM) decreases cell growth (Left panel) and increases apoptosis (Right panel) of the indicated TAL1-positive but not TAL1-negative T-ALL cell lines. Left panel: Viable cell numbers after GSK-J4 treatment relative to viable cell numbers after treatment with vehicle control are reported as mean values +/- s.e.m. (n=3). Right panel: Apoptosis is reported as the percentage of Annexin V positive cells. Data are shown as mean +/- s.e.m. (n=3). $^{**}p < 0.01$; $^{***}p < 0.001$; ns, not significant.

D, Scatter plot summarizing genome-wide changes in gene expression upon GSK-J4 treatment in TAL1-positive Jurkat T-ALL cells (adjusted p-value ≤ 0.05). RNA-seq was performed in duplicate in vehicle-treated and GSK-J4-treated Jurkat cells. Left panel: Genes that are downregulated upon UTX knockdown and are enriched in the GO term category “Cell Cycle” are highlighted in orange. Right panel: Genes that are upregulated

upon UTX knockdown and are enriched in the GO term category "Apoptosis" are highlighted in blue).

E, Dose-dependent effect of GSK-J4 on the induction of apoptosis in primary blasts from TAL1-positive but not TAL1-negative T-ALL patients. FACS plots measuring Annexin V staining are shown for the indicated patients at increasing concentrations of GSK-J4. The plots are representative examples of three biological replicates. Mean data for these patients and for additional patients are shown in Fig. 4A,B.

F, Primary blasts from TAL1-positive and TAL1-negative patients are resistant to treatment with dexamethasone. Primary blasts from T-ALL patients were incubated with increasing concentrations of dexamethasone. Data are presented as mean values of the percentage of CD7-positive AnnexinV-negative cells +/- s.e.m. (n=3).

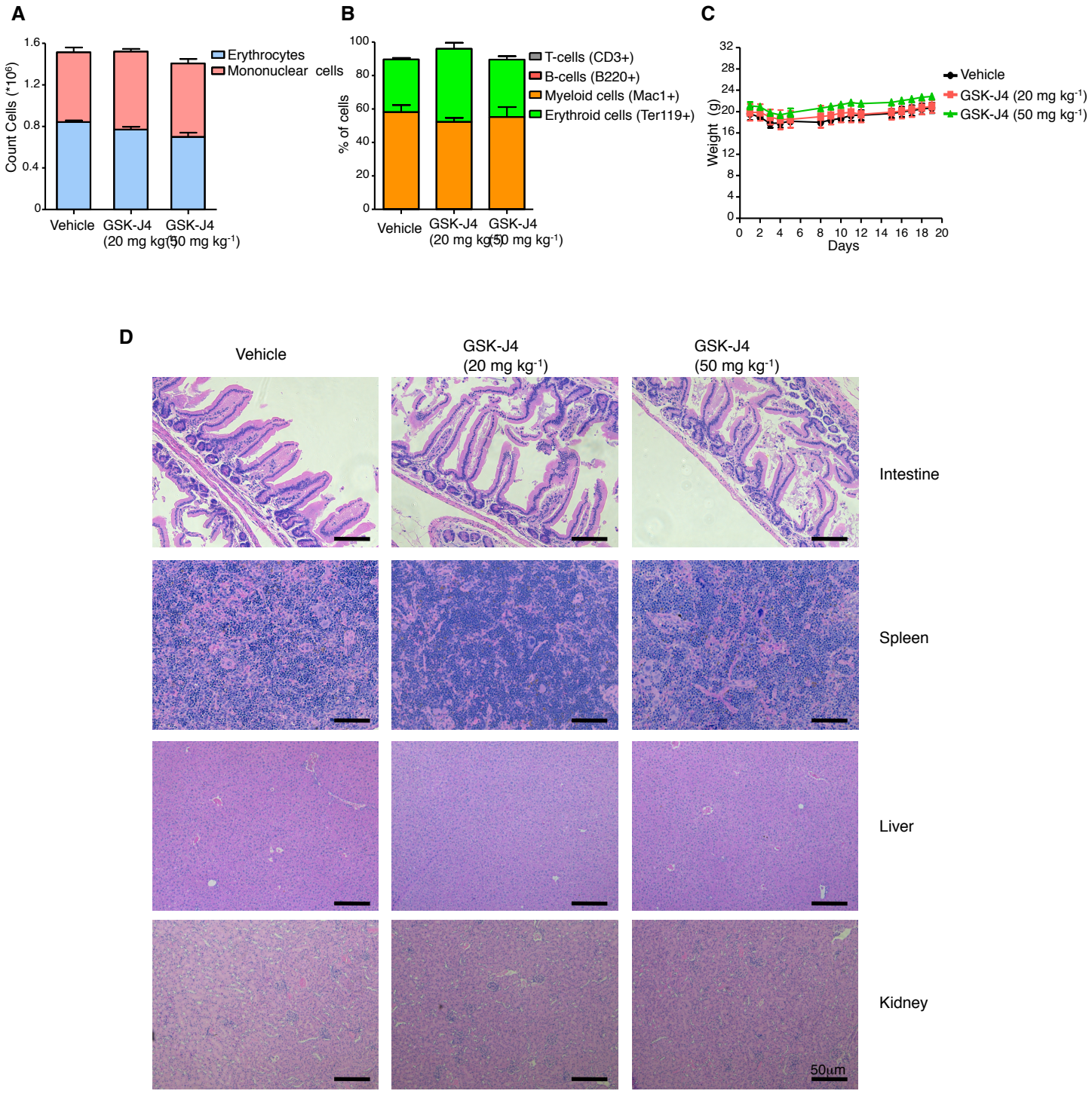
A
Count Cells (*10^6)
1.6
1.2
0.8
0.4
0
Erythrocytes
Mononuclear cells
Vehicle
GSK-J4 (20 mg kg-1)
GSK-J4 (50 mg kg-1)
B
% of cells
100
80
60
40
20
0
T-cells (CD3+)
B-cells (B220+)
Myeloid cells (Mac1+)
Erythroid cells (Ter119+)
Vehicle
GSK-J4 (20 mg kg-1)
GSK-J4 (50 mg kg-1)
C
Weight (g)
32
28
24
20
16
12
8
4
0
0 2 4 6 8 10 12 14 16 18 20
Days
Vehicle
GSK-J4 (20 mg kg-1)
GSK-J4 (50 mg kg-1)
D
Vehicle
GSK-J4 (20 mg kg-1)
GSK-J4 (50 mg kg-1)
Intestine
Spleen
Liver
Kidney
50µm

Supplemental Figure 5. GSK-J4 is well tolerated in mice.

A, **B**, No significant differences in blood cells counts are observed upon GSK-J4 treatment at two different doses. NSG mice were treated with GSK-J4 or a vehicle control as described in Fig. 5A except that mice were not engrafted with leukemic cells. Blood cells were analyzed by FACS with the indicated Abs. Data are presented as mean values +/- s.e.m. (3 mice/group).

C, No significant changes in body weight are observed upon GSK-J4 treatment. Mean values of mice body weights are presented +/- s.e.m. (3 mice/group).

D, No adverse effects are detected in the indicated organs upon GSK-J4 treatment. Histological sections of the intestine, spleen, liver and kidney were taken post-GSK-J4 treatment and stained with haematoxylin and eosin.

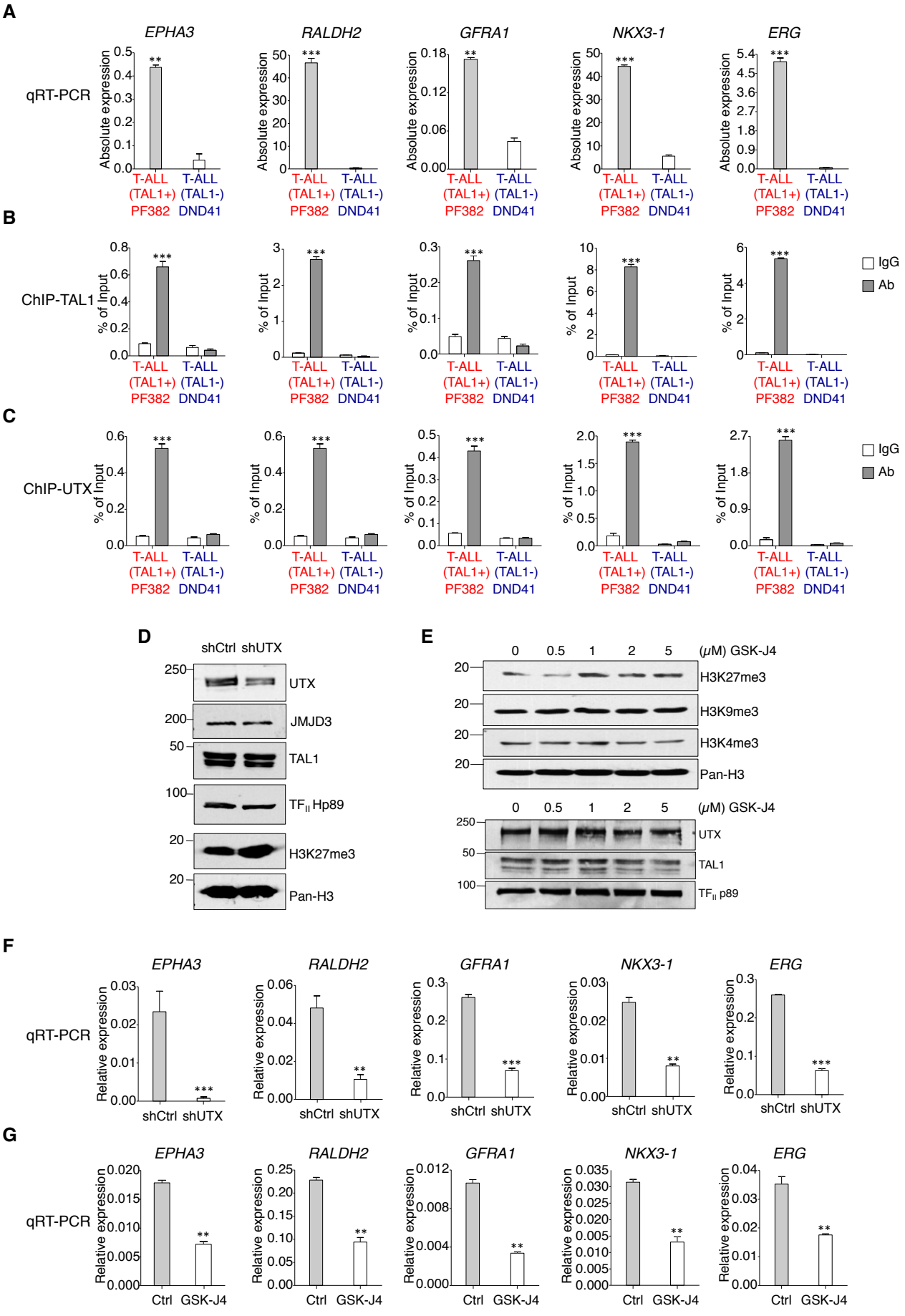
A
EPHA3
RALDH2
GFRA1
NKX3-1
ERG
qRT-PCR
Absolute expression
T-ALL (TAL1+) PF382
T-ALL (TAL1-) DND41
B
ChIP-TAL1
% of Input
IgG
Ab
C
ChIP-UTX
D
shCtrl shUTX
UTX
JMJD3
TAL1
TFII Hp89
H3K27me3
Pan-H3
E
0 0.5 1 2 5 (μM) GSK-J4
H3K27me3
H3K9me3
H3K4me3
Pan-H3
UTX
TAL1
TFII p89
F
Relative expression
shCtrl shUTX
G
Ctrl GSK-J4

Supplemental Figure 6. UTX is enzymatically active and regulates TAL1-target genes in the T-ALL cell line PF-382

A, TAL1-target genes are expressed at higher levels in the TAL1-positive PF-382 cell line compared to the TAL1-negative DND41 cell line.

B, TAL1 is bound to its target genes in the TAL1-positive PF-382 cell line. The TAL1-negative cell line DND41 is used as a negative control.

C, UTX co-occupies TAL1-binding sites in the TAL1-positive PF-382 cell line but is not bound to these sites in the TAL1-negative DND41 cell line.

D, UTX knockdown in PF-382 cells leads to an increase in global levels of H3K27me3, indicating that UTX is enzymatically active.

E, Dose-dependent increase in global levels of H3K27me3 in the PF-382 cell line upon treatment with the H3K27 demethylase inhibitor GSK-J4.

F, **G**, UTX knockdown (**F**) or UTX inhibition via GSK-J4 (**G**) in the PF-382 cell line decreases the expression of TAL1-target genes, indicating that UTX is functionally active as a TAL1 co-activator in these cells.

A, **F**, **G**, Mean qRT-PCR values are presented relative to the internal control *ß2M* +/- s.d. (n=3). **p < 0.01; ***p < 0.001.

B, **C**, Mean ChIP-qPCR values are expressed as a fraction of input +/- s.d. (n=3). ***p < 0.001.

D, **E**, Western blots are representative of three biological replicates. Molecular masses (in kDa) are indicated.

Supplemental Material and Methods

Direct interactions between recombinant proteins

Full-length human TAL1 (Calkhoven et al. 2003) was cloned into pET15b to produce the pET15b-His-TAL1 expression vector. His-tagged TAL1 was expressed in bacteria and purified using TALON His-tag resin (Clontech). Flag-tagged UTX (Wang et al. 2012) was expressed in baculovirus infected Sf-9 cells and purified using M2-Agarose resin (Sigma). Equal amounts (1 μg) of purified His-TAL1 and Flag-UTX proteins were incubated on ice for 2h, followed by TAL1 or UTX IP. After washing, bound proteins were eluted by heating at 95^0C for 5 min. in SDS-containing buffer and analyzed by Western blot. Flag pull down experiments with GST-TAL1 (full length and deletion mutants (Hu et al. 2009)) and purified Flag-tagged UTX were performed as follow. Briefly, 8 μg of purified Flag-UTX and bacterial extract containing an estimated 8 μg GST-TAL1 (or mutants as indicated) were incubated overnight at 4^0C with rotation in the IP 100 buffer (25 mM Tris, pH 7.9, 5mM $MgCl_2$, 10% (v/v) glycerol, 0.1 % (v/v) NP40, 100mM KCl, 0.3 mM DTT and protease inhibitors). Flag beads were added to the mixture and the incubation pursued for 2h. After washing, bound proteins were eluted by heating at 95^0C for 5 min. in SDS-containing buffer and analyzed by Western blot.

Histopathology

Organs were harvested, washed 3 times in phosphate buffered saline (PBS) and immersion-fixed with Formalin (neutral buffered, 10%. ref: HT501128-4L) for 48h at room temperature (RT). Samples were washed 3 times with PBS at RT and dehydrated

by incubation in 50% ethanol for 2h at RT followed by overnight incubation in 70% ethanol at 4°C. Samples were embedded in paraffin blocks. Sections (4-6 μm thick) were stained with hematoxylin and eosin (H&E) following standard procedures. Spleen sections were stained by immunohistochemistry using standard procedures with a human CD45 Ab revealed with a secondary HRP-conjugated Ab.

Apoptosis

Apoptosis was measured by Annexin V staining using the PE Apoptosis Detection Kit I (BD-Pharmingen) as previously described (Palii et al. 2011).

TAL1 and UTX overlap genome-wide in Jurkat cells

To identify UTX/TAL1 co-bound sites we computed the number of TAL1 peaks whose genomic interval intersects with any UTX peak. To estimate the statistical significance of this overlap, we used two approaches:

As a first approach, we used the Fisher Exact test where:

Number of peaks in TAL1-UTX intersection = 2,164

Number of peaks in TAL1 but not UTX = 514

Number of peaks in UTX but not TAL1 = 15,232

Estimated possible peak locations = 159,753 (corresponding to the number of DNAse1 hypersensitive sites in Jurkat cells according to ENCODE).

The Fisher Exact test outputs a p-value of 0.

As a second approach, we repeatedly randomized the locations of each peak, and estimated the probability of the observed intersection size. More specifically, we

repeatedly reassigned each TAL1 and each UTX peak to a new chromosome and starting location, retaining the peak width. In doing so, we ensured that no two moved TAL1 peaks overlapped and no two moved UTX peaks overlapped. (If any did, we reassigned their locations again). We then computed the intersection of the moved peak sets. The average number of overlapping peaks based on 1,000 random shufflings was 8.2720 (compared to 2,164 peaks overlapping in the real TAL1 and UTX locations). The standard deviation was 2.8831. Thus, the observed number of intersecting peaks is approximately 748 standard deviations above the expected amount by random shuffling -- the probability of which by random chance is exceedingly remote.

Based on these two analyses, we estimate that the p-value for the TAL1 UTX overlap is < 0.001.

GSEA analysis

Gene Set Enrichment Analysis (GSEA) (Subramanian et al. 2005) was run using the GSEAPreranked option with 'classic' enrichment scores, as recommended by the authors. The gene set used for scoring comprised expressed genes with a TAL1/UTX co-bound peak in the region spanning 50kb upstream of the TSS to the 3' end of the gene (i.e. defined as "TAL1/UTX co-bound genes"- see Supplemental Table S2) that have significantly decreased expression (adjusted p-value <0.05) in TAL1-knockdown. The ranked expression set was generated from the UTX-knockdown DESeq2 RNA-seq results for protein-coding genes. Ranking for genes with an adjusted p-value < 0.05 was calculated as $log_{10}(\mathrm{p-value}) \times \mathrm{sign}(\mathrm{log2FoldChange})$; genes with an adjusted p-value ≥0.05 were given a rank of zero. This analysis is shown in Fig. 2H.

Gene signature correlation

Correlation between UTX-knockdown and GSK-J4 RNA-seq used the R cor.test function to calculate the Pearson product-moment correlation between protein-coding genes that are significantly changed (adjusted p-value <0.05) under both treatments, and to test whether the correlation is significantly different from zero.

Gene Ontology analyses

Genes significantly up- or down- regulated in the shUTX treatment (adjusted p-value ≤ 0.05) were submitted to DAVID Gene Ontology Analysis version 6.7 (Huang da et al. 2009). Results from DAVID were then imported with the EnrichmentMap plugin (Merico et al. 2010) into Cytoscape version 3.2.1 (Shannon et al. 2003) for visualization.

Antibodies

For IP, we used: anti-TAL1 Ab (sc-12984) from Santa Cruz Biotechnology, and antigen-purified anti-UTX Ab (Chaturvedi et al. 2009; Seenundun et al. 2010). For UTX ChIP, we used a 1:1 (v/v) mixture of anti-UTX Ab (Chaturvedi et al. 2009; Seenundun et al. 2010) and commercial anti-UTX Ab (A302-374A) from Bethyl. For anti-H3K27me3 ChIP we used the H3K27me3 Ab (07-449) from Millipore. For immunohistochemistry, we used anti-hCD45 (ab10559) from Abcam. For Western blot, we used: anti-TAL1 from Millipore (clone BTL73); anti-$TF_{II}Hp89$ from Santa Cruz (sc-20697); and anti- RBBP5 (A300-109A) and NCOA6 (A300-410A) from Bethyl. In-house generated anti-ASH2L (#1025) (Demers et al. 2007), anti-PTIP, -PA1 and -WDR5 (Cho et al. 2007) Abs were

described previously. Rabbit anti-JMJD3 Ab was generated against murine His-tagged JMJD3 (aa 902-1048) purified against the antigen and tested for specificity by Western blot after JMJD3 knockdown.

Primers

For ChIP-qPCR:

RALDH2 5'cagggaacactctcccactc3' and 5'tgataagcagccagtcaacg3'

NKX3.1 5'caaccgtcttgctgaggttt3' and 5'ggttagcatctgcattgcac3'

CD226 5'caggcattgaaggctatagga3' and 5'gcttaaaagacaggtttgctgg3'

MYB 5'ccttccccccttccttagaca3' and 5'cctgtttcctgtttgggaga3'

ERG 5'cctcctcttaacggctgatg3' and 5'atcagggctgaacactcgtt3'

PDGFC 5'tgtggctcctttgtcactt3' and 5'gctccttgagctgctgat3'

GFRA1 5'cagactctgtggtctaagcatc3' and 5'ctaccctgctctcatgtcattt3'

EPHA3 5'tgttggacggttcttctgtt3' and 5'tcagagagaagtgtgtagttagaatg3'

For qRT-PCR:

RALDH2 5'tgcattcacagggtctactga3' and 5'ttttgcctccaagttccaga3'

NKX3.1 5'agaacgaccagctgagcac3' and 5'taagaccccaagtgcctttc3'

CD226 5'gctttaccgctgctacttgc3' and 5'tccagccacaaagagggtat3'

MYB 5'aattgactgttacaacaccatttca3' and 5'tggggatgtcagaagaggtc3'

B2M 5'cacagcccaagatagttaagt3' and 5'ccagccctcctagagc3'

ERG 5'aacgagcgcagagttatcgt3' and 5'cgtctggaaggccatattct3'

PDGFC 5'cagcaacaaggaacagaacg3' and 5'tgggctgtgaatacttccatt3'

GFRA1 5' ttactggagcatgtaccagagc3' and 5'ccggaatatatctgacaatctgc3'

EPHA3	5’ttttggcaatgggcattta3’ and 5’ggtcttcatatgtatgtgggtcaa3’
PLK1	5’aaccgagttattcatcgagacc3’ and 5’ ttggttgccagtccaaaatc3’
CDK6	5’ tgatcaactaggaaaaatcttgga3’ and 5’ ggcaacatctctaggccagt3’
CUL4A	5’ggacctcgcacagatgtacc3’ and 5’cgatcgctgttccaaaagtc3’
CDCA2	5’cctttggcacaagattctcc3’ and 5’tgactggaaggctgatattcg3’
CDCA8	5’gctgacagcaaagagatcttcc3’ and 5’gccaataatcgcaggctct3’
CDK1	5’tggatctgaagaaatacttggattcta3’ and 5’caatcccctgtaggatttgg3’
CCNB2	5’gaagattgggagaaccctca3’ and 5’tgtgggtttatggactgcaa3’
GTSE1	5’cgatccctgttccaaacaa3’ and 5’ccttgcgagattgctggtag3’
CCNA2	5’ggtactgaagtccgggaacc3’ and 5’gaagatccttaaggggtgcaa3’
AEN	5’tgcagaccggaagagacac3’ and 5’ggaagcctggggagtaatct3’
TP53	5’aggccttggaactcaaggat3’ and 5’ccctttttggacttcaggtg3’
CASP1	5’gcgaagcatactttcagtttca3’ and 5’tctccttcaggaccttgtcg3’
CASP10	5’ggcaaaataagcatgcaggt3’ and 5’gagtgttagcagatgctccttg3’
HRK	5’tactggccttggctgtgc3’ and 5’cacagggttttcaccaacct3’
JUN	5’tctgcatcatctgtagatcctagtct3’ and 5’tgagagtgattttatcgagcattc3’
BBC3	5’gacctcaacgcacagtacga3’ and 5’gagattgtacaggaccctcca3’
CASP4	5’gaatctgagagcccagggatatg3’ and 5’ccatgagacatgagtaccaagaa3’

Supplemental References

Calkhoven CF, Muller C, Martin R, Krosl G, Pietsch H, Hoang T, Leutz A. 2003. Translational control of SCL-isoform expression in hematopoietic lineage choice. *Genes Dev* **17**: 959-964.

Chaturvedi CP, Hosey AM, Palii C, Perez-Iratxeta C, Nakatani Y, Ranish JA, Dilworth FJ, Brand M. 2009. Dual role for the methyltransferase G9a in the maintenance of beta-globin gene transcription in adult erythroid cells. *Proc Natl Acad Sci U S A* **106**: 18303-18308.

Cho YW, Hong T, Hong S, Guo H, Yu H, Kim D, Guszczynski T, Dressler GR, Copeland TD, Kalkum M et al. 2007. PTIP associates with MLL3- and MLL4-containing histone H3 lysine 4 methyltransferase complex. *J Biol Chem* **282**: 20395-20406.

Demers C, Chaturvedi CP, Ranish JA, Juban G, Lai P, Morle F, Aebersold R, Dilworth FJ, Groudine M, Brand M. 2007. Activator-mediated recruitment of the MLL2 methyltransferase complex to the beta-globin locus. *Mol Cell* **27**: 573-584.

Hu X, Li X, Valverde K, Fu X, Noguchi C, Qiu Y, Huang S. 2009. LSD1-mediated epigenetic modification is required for TAL1 function and hematopoiesis. *Proc Natl Acad Sci U S A* **106**: 10141-10146.

Huang da W, Sherman BT, Lempicki RA. 2009. Bioinformatics enrichment tools: paths toward the comprehensive functional analysis of large gene lists. *Nucleic Acids Res* **37**: 1-13.

Merico D, Isserlin R, Stueker O, Emili A, Bader GD. 2010. Enrichment map: a network-based method for gene-set enrichment visualization and interpretation. *PLoS One* **5**: e13984.

Palii CG, Perez-Iratxeta C, Yao Z, Cao Y, Dai F, Davison J, Atkins H, Allan D, Dilworth FJ, Gentleman R et al. 2011. Differential genomic targeting of the transcription factor TAL1 in alternate haematopoietic lineages. *EMBO J* **30**: 494-509.

Seenundun S, Rampalli S, Liu QC, Aziz A, Palii C, Hong S, Blais A, Brand M, Ge K, Dilworth FJ. 2010. UTX mediates demethylation of H3K27me3 at muscle-specific genes during myogenesis. *EMBO J* **29**: 1401-1411.

Shannon P, Markiel A, Ozier O, Baliga NS, Wang JT, Ramage D, Amin N, Schwikowski B, Ideker T. 2003. Cytoscape: a software environment for integrated models of biomolecular interaction networks. *Genome Res* **13**: 2498-2504.

Subramanian A, Tamayo P, Mootha VK, Mukherjee S, Ebert BL, Gillette MA, Paulovich A, Pomeroy SL, Golub TR, Lander ES et al. 2005. Gene set enrichment analysis: a knowledge-based approach for interpreting genome-wide expression profiles. *Proc Natl Acad Sci U S A* **102**: 15545-15550.

Wang C, Lee JE, Cho YW, Xiao Y, Jin Q, Liu C, Ge K. 2012. UTX regulates mesoderm differentiation of embryonic stem cells independent of H3K27 demethylase activity. *Proc Natl Acad Sci U S A* **109**: 15324-15329.